



## Laboratory testing of compressive and tensile strength on level ice and ridged ice from Svalbard region

Victoria Bonath <sup>1</sup>, Aniket Patil <sup>2</sup>, Lennart Fransson <sup>1</sup>, Bjørnar Sand <sup>2</sup>

<sup>1</sup> Luleå University of Technology, Luleå, SWEDEN

<sup>2</sup> Northern Research Institute, Narvik, NORWAY

### ABSTRACT

Compression and tensile strength properties are important input data for constitutive modelling. Still strength properties of ridged ice are not yet sufficiently investigated. During winter 2011 and 2012 field trips were performed to the Svalbard region with the aim to investigate structure and strength of pressure ridges. Core samples from different ridges and the surrounding level ice were taken and transported to the laboratory at Luleå University of Technology. Studies on thin sections of the ice samples under cross-polarized light delivered information about internal structure of the ice. Uniaxial compressive and tensile strength tests were performed with horizontal and vertical loading directions. The experimental procedure is explained in detail. Salinity and porosity were measured for each sample. In this paper the mechanical properties obtained from the testing are documented by consideration of crystal type, ice depth and total porosity.

### INTRODUCTION

The presence of sea ice ridges are one of the major challenges when it comes to ice-structure-interaction and ice navigation. Especially the high frequency of their occurrence increases the importance of taking ridges into account whenever it comes to an offshore engineering issue in ice affected waters. Leppäranta (2011) states that an average volume of ridged ice accounts for 10 to 40% of total sea ice volume. Strub-Klein and Sudom (2011) summarised data on morphological properties of over 300 first-year ridges in the arctic and subarctic regions collected between 1971 and 2011. In general they found a high spatial variation on ridge geometry, especially for sail and keel dimensions and consolidated layer thickness. Further they concluded a lack of data on physical and mechanical properties of sea ice ridges. Even though mechanical properties of sea ice ridges have been studied for many years and reasonable approaches have been found there is still a potential need for further studies. In order to improve numerical models for simulating ridge loads on offshore structures a good approach for typical behaviour and geometry of ice ridges for different areas has to be found. The problematic accessibility of arctic offshore regions and the complexity involved in arctic research expeditions limits the amount of data to a minimum necessary extent. Every additional data from further expeditions are of high value in order to either confirm or optimize the state of knowledge.

Ice ridges can be divided into sail and keel. In first-year ice ridges, the keel consists of a consolidated layer and unconsolidated rubble below (WMO, 1970). The strength of both keel and sail can be characterized by freeze bond strength between the contact areas of the ice blocks. The highest load impact is released from the consolidated layer which often is assumed to behave as level ice. Anyhow the consolidated layer consists of refrozen crushed ice mixed with refrozen slush. Unlike for level ice, the ice growth is disturbed by ridge

building actions and thus the ice crystal structure cannot be assumed to consist of mainly vertical columns with some granular ice on the top.

Four types of failure modes for ridges were described by Bonnemaire and Bjerkås (2004) during observations of ridge-structure-interaction with the lighthouse Norströmsgrund in the Gulf of Bothnia. Crushing and bending were the dominating reasons for failure. Considering that ice is generally weaker in tension (Mellor, 1983), the tensile strength may be the limiting factor in many cases of bending failure.

Høyland (2007) concluded from a detailed study of ridges in the Barents Sea that uniaxial compressive strength of the consolidated layer is generally in between the horizontal and vertical compressive strength due to differences in the crystal structure.

Shafrova and Høyland (2008) presented spatial compressive strength distribution charts on two first-year ridges in the Barents Sea and in the Arctic Ocean, based on uniaxial compressive strength tests. They found that ratio of horizontal to vertical strength was 2 for level ice and 1.1 for the consolidated layer and ice rubble. Compressive strength for the ice rubble in the keel was noticeable low with an average value lower than 0.5 MPa at ice temperatures of approximately  $-1.6^{\circ}\text{C}$ .

Even though some work has been done on testing tensile strength of level ice in laboratory, not many tests have been performed, which may be based on the complexity of testing procedure and time requirements. Timco and Weeks (2010) summarized a number of uniaxial tensile strength tests in horizontal loading direction and presented the data as a function of total porosity. All values were within 0.2 and 0.8 MPa.

During two expeditions in March 2011 and in March 2012 with the Norwegian coastguard vessel KV Svalbard, pressure ridges around Svalbard and in the Fram Strait has been studied with respect to ridge geometry and physical and mechanical properties. Sand et al. (2013) describe the location and morphology of the studied ridges. A number of ice samples from the ridges and from level ice have been taken and transported to Luleå University of technology. Ice rubble was taken into account during profiling but no strength tests were performed on the rubble. Ice strength was tested by uniaxial tension and compression in both vertical and horizontal loading directions. The crystal structure was observed and salinity and density of the ice was measured with respect to the depth of the ice sample.

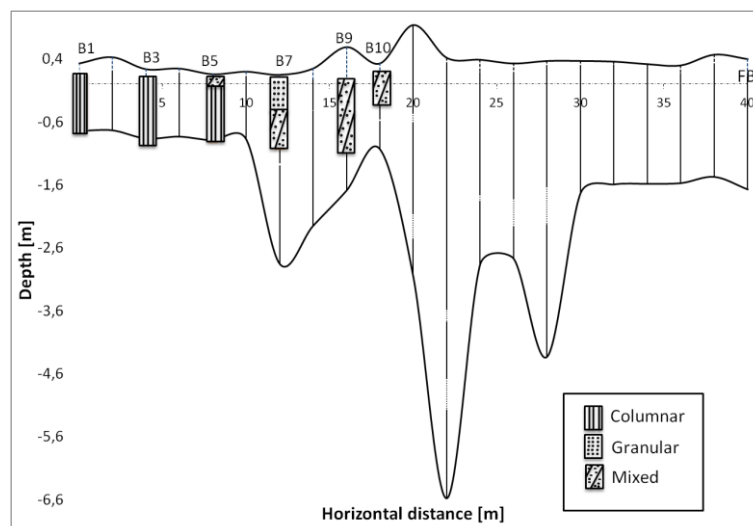


Figure 1. Ridge profile and ice sample location for the studied ridge in 2012. The samples are hatched with respect to crystal type.

## METHOD AND EXPERIMENTAL SET-UP

### *Sampling*

All the cores were taken with a 200 mm drill auger from both level ice and the profiled cross-sections of the pressure ridges. While the samples from 2011 are from random locations within the ridge, the sample location is well known within the ridge profile for the cores taken during 2012 as shown in Figure 1. The ice samples were stored in a cold container at  $-20^{\circ}\text{C}$  and transported to the laboratory at Luleå University of Technology (LTU).

### *Crystal study*

Since the crystal structure of ice is an important factor for ice properties, thin ice sections were prepared in horizontal and vertical direction for each specimen. Photographs were taken from all sections using cross-polarised light. Each specimen could be classified into ice type (granular, columnar and mixed) and grain size and orientation.

### *Setup compression tests*

The loading machine used at LTU consists of a servo-hydraulic cylinder controlled by a closed-loop system. A load cell is installed above the specimen and deformation is measured below the specimen. The test rig is placed into a small cold chamber to keep the chosen sample temperature during the test. Steel plates are used as contact plates. During the test series in 2011 horizontal tests were performed on cylindrical specimen. The cylindrical cores were prepared with a coring drill with a diameter of 7cm. For vertical strength tests the specimens were cut with a band saw into cuboids with a square loading area. Side length was 70 mm and sample height was 170 mm. For the tests in 2012 all samples were chosen to be cuboids with about the same dimensions as 2011. Smoothing of the contact surfaces at the specimen shall diminish radial restraint from the steel plates; anyhow this affect cannot be completely eliminated. All samples were tested at  $-10^{\circ}\text{C}$  and a strain rate of  $10^{-3} \text{ s}^{-1}$ .

### *Setup tensile tests*

Uniaxial tensile strength was determined through direct tension. The same loading machine was used as for the compression tests. The load was transferred through wedge-shaped end holders. Specimens with a rectangular cross section as shown in Figure 2 were cut with a band saw. The ends of the specimen were enlarged so that they fit into the end holder. High accuracy was required during sample preparation. After the first test series on the Svalbard ice from 2011, both the specimen shape and the end holders were optimised in order to prevent stress concentrations in the ice at the bearings. The end holders were rounded at the contact edges and the specimen was shaped with a radius reducing the cross-section area towards the centre. All specimens were tested at  $-10^{\circ}\text{C}$ . Constant loading speeds between 0.01 mm/s and 0.1 mm/s were applied. Unlike most of the samples from 2011, almost all samples failed in the middle of the test section during testing in 2012.

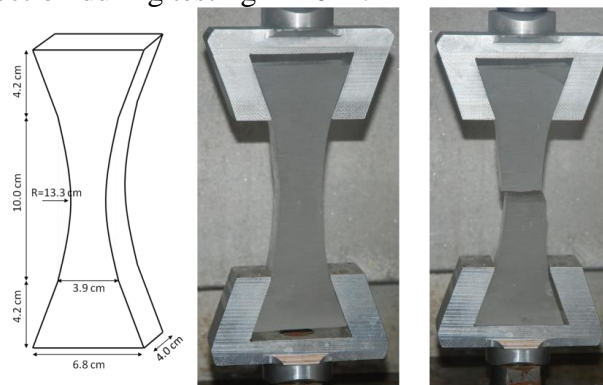


Figure 2. a) Specimen dimension for tensile tests 2012. b) Specimen loaded in tension before failure. c) Specimen failed under uniaxial tensile load.

### ***Salinity and Porosity***

Density was determined by dividing weight through volume. Accurate values for geometry and weight were measured just before testing the samples. Density measurements were not done on the tensile specimen from 2011. After testing the samples they were melted and salinity could be determined. A widely recognised empirical approach was used to calculate brine volume and air volume (Cox and Weeks, 1983). The same approach to determine total porosity was used by Shafrova and Hoyland (2007) and Moslet (2006) for their compression tests, which amongst others will be used as comparative data for these results.

Table 1. Overview on ice tests during 2011 and 2012. Loading type and direction, number of specimen and average values for strength, salinity and density are summarized.

Samples 2011					
Load	Direction	Salinity [ppt]	Density (kg/m <sup>3</sup> )	n	$\bar{\sigma}$ (MPa)
Compression (Ridge)	Hor	4.57	881.4	50	4.35
Compression (Ridge)	Ver	3.31	871.7	12	4.17
Tension (Ridge)	Hor	4.17	-	37	0.31
Tension (Ridge)	Ver	4.17	-	34	0.29
Samples 2012					
Load	Direction	Salinity [ppt]	Density (kg/m <sup>3</sup> )	n	$\bar{\sigma}$ (MPa)
Compression (Level ice)	Hor	2.95	893.8	22	5.18
Compression (Ridge)	Hor	3.94	883.1	31	3.88
Compression (Ridge)	Ver	5.15	891.3	20	8.56
Tension (Ridge)	Hor	3.21	885.5	35	0.42

## **RESULTS**

### ***Crystal structure***

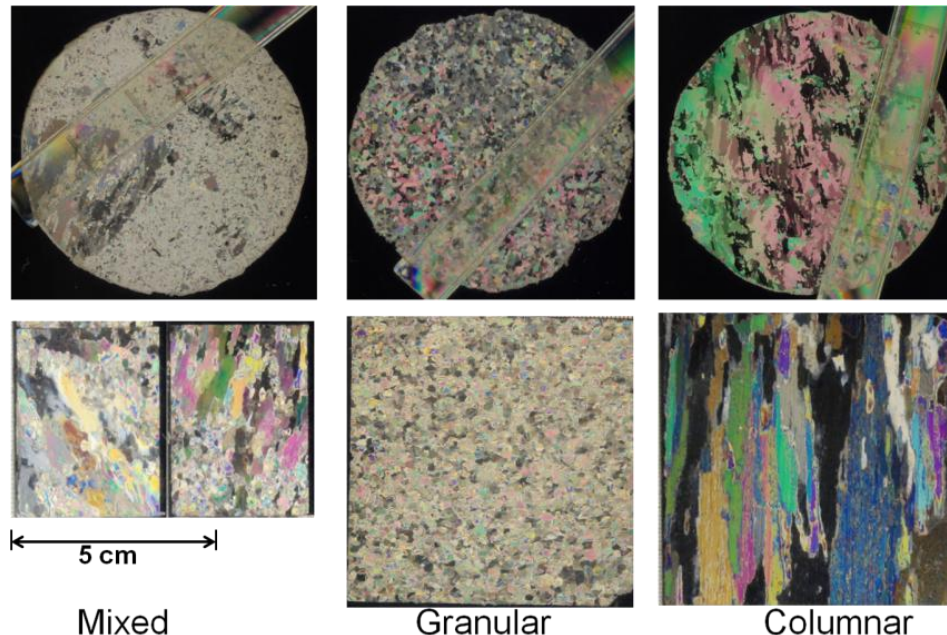


Figure 3. Examples for horizontal and vertical thin sections for mixed, granular and columnar ice.

All ice specimens were classified into ice type regarding shape and mixture of ice crystals. Figure 3 shows horizontal and vertical thin sections for typical examples of mixed, granular and columnar ice. For the ice from the ridges 172 of 219 were classified as mixed type. The distribution of ice type in the ridge profile from 2012 is shown in Figure 1. For the samples

from level ice mainly columnar ice was found in the deeper layers. The upper parts of the cores consisted of mixed ice. Regarding crystal structure and the salinity profile shown in Figure the 4a, the level ice can be a matter of multiyear ice, with melted and refrozen snow ice on top.

### Physical properties

Figures 4a and 4b show depth profiles of salinity and porosity for the samples taken in 2012. The level ice had almost no salt content at the top of the ice, but increasing salinity towards depth. For ice from the consolidated layer salt content was highest on the top. In average salinity and total porosity were decreasing until a depth of 0.5 m and almost constant then.

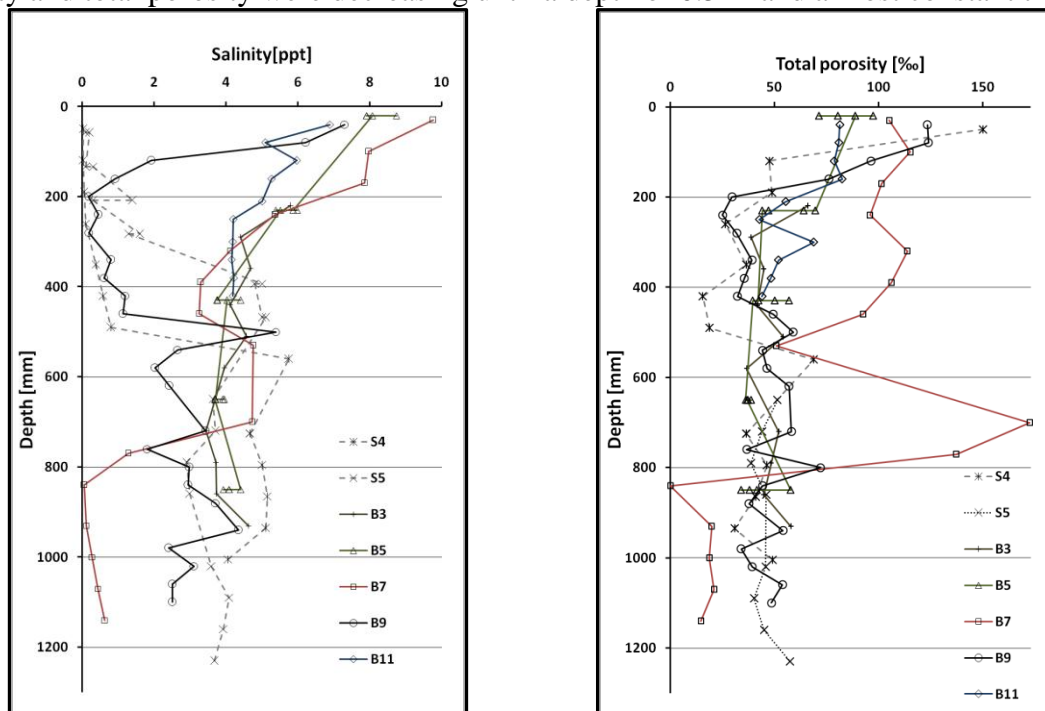


Figure 4. Profiles of a) salinity and b) total porosity for the Svalbard ice 2012.

### Uniaxial compressive strength

The results for compressive strength with respect to the total porosity are summarised in Table 2. A relationship between total porosity and ice strength could be clearly observed, with higher strength values for lower porosities. The ice from 2012 was weaker in horizontal loading than in vertical loading. This observation is not valid during 2011, where the ice structure solely was of mixed or granular type. Figures 5 and 6 show a strength frequency distribution for respectively load direction for all tests. A normal strength distribution could be found for horizontal loading whereas strength was distributed randomly for vertically loaded specimen. Information about the crystal type-strength dependency is shown in figure 9. The results of the crystal study are listed in table 4. Failure type is brittle for all vertical samples except of two. Ductile failure was clearly dominating for horizontal loading. Brittle failure was observed for 15% of all horizontal specimens.

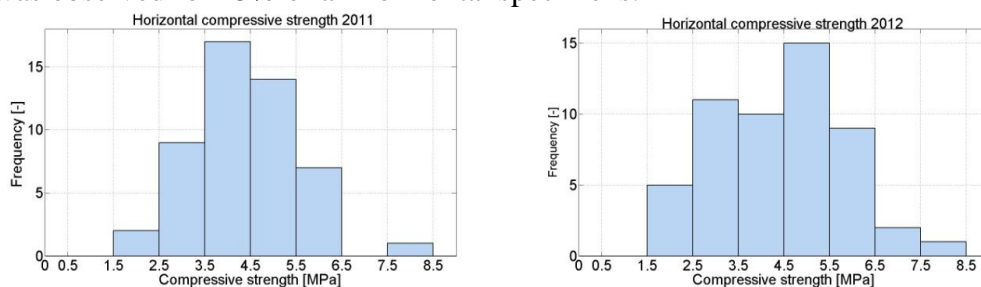


Figure 5. Frequency distributions of horizontal compressive strength.

Table 2. Results from horizontal and vertical compressive strength tests with respect to different ranges of total porosity for both ridge and level ice.

Samples 2011							
Ridge - horizontal			Ridge - vertical				
$\nu_t$ (‰)	$\sigma_{ch} \pm stdev$ (MPa)	n	$\sigma_{cv} \pm stdev$ (MPa)	n			
0-25	5.46±0.59	3	5.91±0.00	1			
25-50	4.87±2.05	6	4.77±0.67	2			
50-75	4.43±1.14	16	4.76±1.49	2			
75-100	3.87±1.18	7	4.06±1.63	3			
100-125	3.74±0.46	3	3.23±0.01	2			
Samples 2012							
Ridge - horizontal			Ridge - vertical		Level ice – horizontal		
$\nu_t$ (‰)	$\sigma_{ch} \pm stdev$ (MPa)	n	$\sigma_{cv} \pm stdev$ (MPa)	n	$\sigma_{ch} \pm stdev$ (MPa)	n	
0-25	5.57±1.71	5	-	-	4.43±1.20	2	
25-50	4.04±0.88	8	9.93±3.07	12	5.48±0.94	16	
50-75	3.88±1.21	8	6.17±1.82	5	5.15±1.09	3	
75-100	3.15±1.39	3	6.18±1.05	3	-	-	
100-150	2.51±0.68	6	-	-	-	-	
150-200	3.03±0	1	-	-	2.04±0	1	

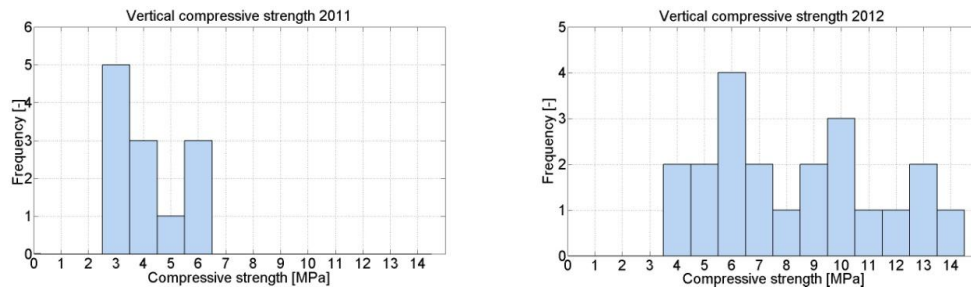


Figure 6. Frequency distributions of vertical compressive strength.

### Uniaxial tensile strength

Tensile strength tests are not comparable between testing periods 2011 and 2012 since the end holders and specimen shape were slightly changed after the first test series. A crystal study showed that all specimens for both test series had mixed ice type. In 2011 the mean strength is 0.36 MPa for loading speed of 0.01 mm/s and 0.29 MPa for 0.02 mm/s. It has to be mentioned that average salinity for the former is 1.91 ppt whereas average salinity for the latter is significantly higher with 4.52 ppt. Tensile strength versus salinity is plotted in Figure 10a. In 2012 the average tensile strength is higher with 0.42 MPa. Table 3 shows tensile strength with respect to total porosities for test series 2012.

Table 3. Average tensile strength grouped into different ranges of total porosity.

Samples 2012		
$\nu_t$ (‰)	$\sigma_{th} \pm stdev$	n
25-50	0.45±0.16	18
50-75	0.42±0.42	9
75-100	0.36±0.36	6
100-125	0.43±0.12	2

## ANALYSIS

### *Uniaxial compressive strength versus total porosity*

Expressing ice strength as a function of strain rate and total porosity was suggested by Timco and Frederking (1990). They presented this relationship for different crystal types, loading directions and strain rates between  $10^{-7}$  and  $10^{-4} \text{ s}^{-1}$  at which ductile failure of ice is expected. Since most of our samples showed ductile material behaviour, this approach might be applicable even at a strain rate of  $10^{-3} \text{ s}^{-1}$ . Anyhow a fit of the data was not successful. Moslet (2007) suggested an approach expressing maximum strength which can be written as in Eq.1.

$$\sigma_c = A \left( 1 - \sqrt{\frac{V_T}{B}} \right)^2 \quad (1)$$

For the limiting porosity (B) at which sea ice loses its strength, 0.7 is chosen. Empirical values for parameter A are 8 MPa for horizontal and 24 MPa for vertical loading. These functions are fitted by try and error principle to in total 540 tested specimen of columnar sea ice. Shafrova and Hoyland (2008) used the same function after testing 376 specimen from both level ice, consolidated layer and ice rubble, yet when fitting to their maximum values A became 10.5 MPa and 5.25 MPa for vertical and horizontal strength in level ice and 9.1 MPa and 7 MPa respectively for ice from the consolidated layer. Even though only a small number of vertical tests were performed, Moslet's (2007) approach is valid for our data, as can be seen in Figure 7b. Regarding horizontal strength, Figure 7a shows that our data are clearly higher and a new parameter A equal to 10.3 MPa is representative for this study. Shafrova and Hoyland (2008) stated that enhanced brine drainage in horizontal specimen, as earlier described by Hoyland (2007), resulted in higher total porosities and thus lower strength. This effect was diminished in this study since both air temperature while sampling and storage temperature were  $-20^\circ\text{C}$  and colder. Further average testing temperature was much lower. Unlike Shafrova and Hoyland (2008) the maximum strength for level ice was higher than for ice in the consolidated layer in 2012.

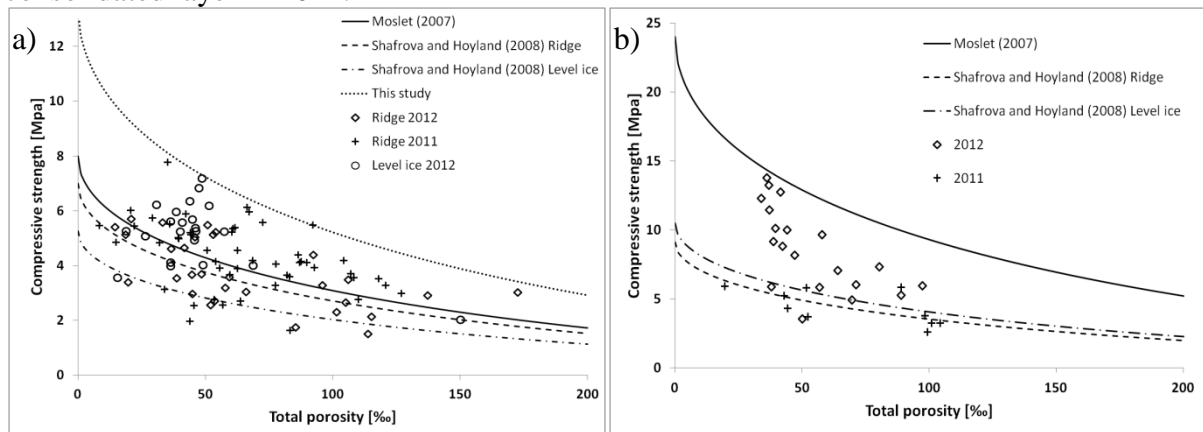


Figure 7. a) Horizontal and b) vertical compressive strength for all tested specimen. The level ice samples are marked with a circle; all other samples are from consolidated layer. Trend lines expressing maximum compressive strength are added from earlier studies.

### *Uniaxial compressive strength for different crystal types*

By analysing the crystal structure profiles from each borehole from the ridge 2012, it was found that the closer the samples were located to the centreline of the ridge, the more ice with a mix of columnar and granular grains can be expected. This can be an important factor for modelling ridge loads against structures, since material behaviour is changing. Instead of the assumed anisotropic columnar ice in the consolidated layer, material properties approach isotropic behaviour, depending on the total amount of mixed ice and the ratio and distribution between different ice types. In 2012 61% of the samples from ridge were classified as mixed

ice, in 2011 even 90% of the specimen were of mixed type. The higher value for 2011 probably is a result from both the thinner ice sheets from which the ridge was built and a more moderate climate. Less force is required to separate the sheet into smaller ice pieces and distribute them randomly. The ratio between vertical and horizontal compressive strength is given in Table 4. The fact that the ratio for mixed ice in 2012 is higher depends on the average vertical compressive strength which is 2 MPa higher than in 2011. By studying the texture of the samples it could be found that the content of granular grains was lower in 2012 and the portion of columnar grains was oriented with the long axis vertically. Finally mixed ice had highest average compressive strength in horizontal direction and columnar ice had significantly a higher average strength in vertical direction.

Table 4. Average horizontal and vertical strength for different ice types with respectively average porosity. Ratios between vertical and horizontal strength are denoted.

Samples 2011							
Ice type	Horizontal load			Vertical load			Ratio $\sigma_{cv}/\sigma_{ch}$ (-)
	$\sigma_{ch} \pm stdev$ (MPa)	$v_t$ (‰)	n	$\sigma_{cv} \pm stdev$ (MPa)	$v_t$ (‰)	n	
Granular	3.96±1.19	78.49±29.82	13	-	-	-	-
Columnar	-	-	-	-	-	-	-
Mixed	4.48±1.23	58.87±27.13	37	4.17±1.21	70.19±31.14	12	0.93
Samples 2012							
Granular	3.90±1.90	89.46±33.59	12	-	-	-	-
Columnar	4.21±1.20	46.82±15.67	18	9.16±3.11	45.81±10.84	16	2.18
Mixed	4.86±1.36	47.11±37.80	23	6.14±0.86	84.45±11.22	4	1.26

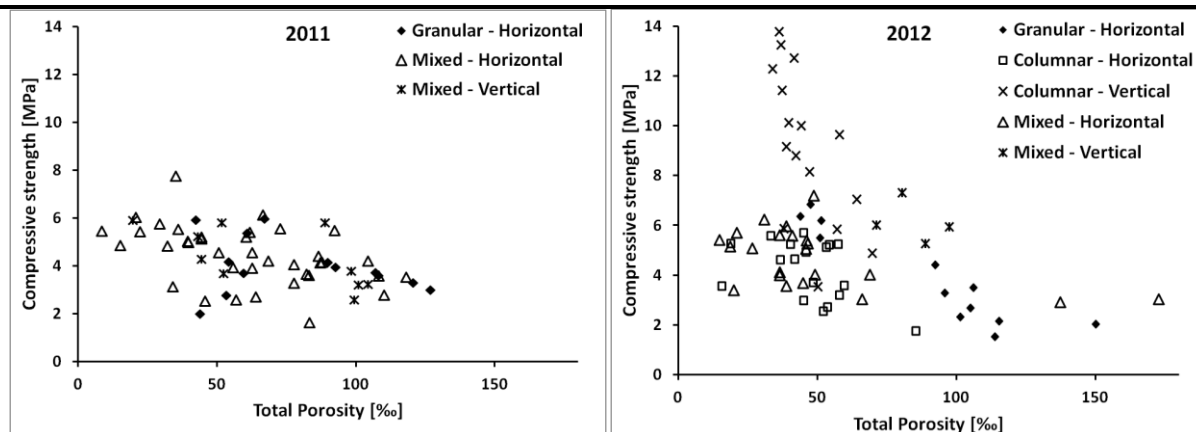


Figure 8. Compressive strength vs. total porosity for resp. ice type and load direction for the years 2011 and 2012.

### Uniaxial tensile strength

Direct tensile tests were performed during both years. In 2011 many of the samples failed at the contact edge of the specimen holder due to local load concentrations. This effect can be observed as in Figure 9. A clear peak at a tensile strength of 0.2 MPa appears in 2011. In 2012 approximately a normal maximum strength distribution can be assumed.

Two different constant loading speeds were applied for this series. The average strength at 0.01 mm/s is slightly higher than for 0.02 mm/s. This difference can as well be attributed to the much higher average salinity for the latter. Richter-Menge and Jones (1993) found after a number of tensile strength tests with varying load rates that this parameter has a significantly lower impact on the tensile strength compared to parameters such as temperature and salinity. In Figure 10a all results from tensile testing are summarized and plotted against salinity. A trend of nonlinear relationship between these parameters can be observed, where average tensile strength is higher for low salinities. No trend can be observed for different loading

speeds. The loading speed is anyway not comparative for the two testing years since two different methods were used. All results are in a range between 0.1 and 0.9 MPa. This range was also found by Timco and Weeks (2010) when they summarized results of a number of horizontal direct small-scale tensile tests that have been done between the years 1970 and 1993. Their attempt to fit the data for horizontal tensile strength ( $\sigma_t$ ) regarding total porosity ( $v_T$ ) yielded in a Eq. 2 which is plotted in Figure 10b.

$$\sigma_t = 4.278v_T^{-0.6455} \quad (2)$$

Compared to our results from 2012 this formula slightly underestimates the tensile strength. Several reasons come into consideration. The testing methods differ for different data sets. The number of tests performed is small in both Timco and Weeks (2009) function and in our test series. All specimens have a mixed ice type and columns are randomly directed within granular ice whereas the results used by Timco and Weeks (2009) refer to columnar first year ice with horizontal loading direction. Columnar ice has higher tensile strength in vertical loading direction which amongst others was shown by Sammonds et al. (1998).

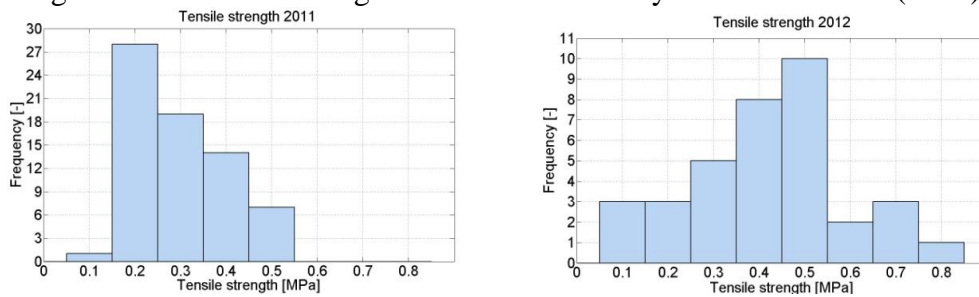


Figure 9. Frequency distributions of uniaxial tensile strength.

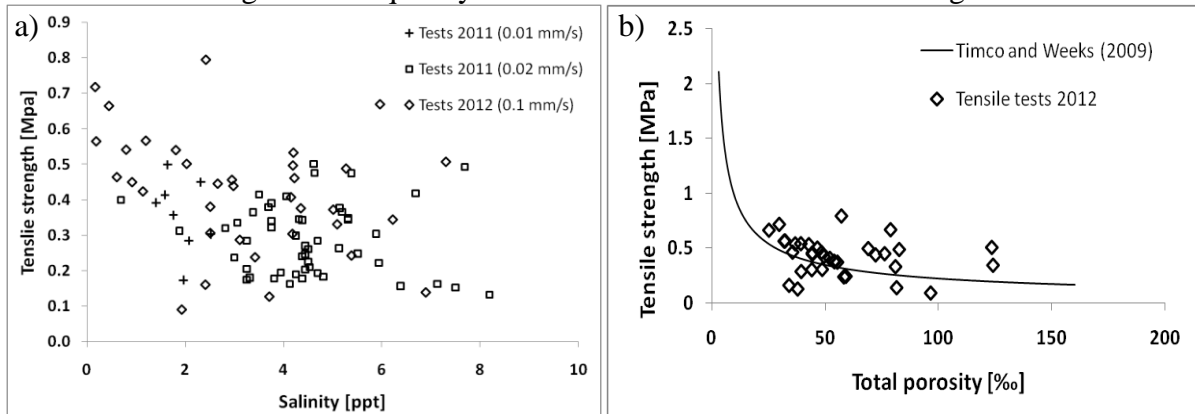


Figure 10 . Tensile strength is plotted versus a) salinity for all specimen and versus b) total porosity for specimen from 2012 with a data fit from Timco and Weeks (2010).

## CONCLUSIONS

In total 135 uniaxial compression and 106 uniaxial tension tests were performed during 2011 and 2012 from both ridged and level ice. All samples were tested at  $-10^{\circ}\text{C}$ . Crystal type, density and salinity were determined.

- About 80% of the tested samples from the ridge could be identified as mixed ice texture. The closer the sample was located to the centreline of the ridge, the more mixed ice could be found.
- The ratio between horizontal and vertical compressive strength was 2.18 for columnar ice and between 0.93 and 1.26 for mixed ice. This ratio varied for mixed ice because of different proportions of granular ice, vertical columns and horizontal columns. Mixed ice was strongest in horizontal compressive loading and columnar ice was strongest in vertical loading direction.

- The uniaxial tensile strength was tested on 71 specimens in 2011 and 35 specimen in 2012. The average strength was 0.30 MPa and 0.42 MPa respectively. The lower value from the first test series was due to contact load concentrations at the specimen holder.
- A relationship can be observed between tensile strengths and salinity. Total porosity did not show a direct influence on tensile strength in this study, a low quantity of specimen maybe the reason. More work is required on tensile strength testing of ice.

## REFERENCES

- Bonnemaire, B. and Bjerkås, M., 2004. Ice ridge-structure interaction, part I: geometry and failure modes of ice ridges. *Proceedings of the 17th International Symposium on Ice, IAHR, Saint Petersburg, Russian Federation* (Vol. 1, pp 123-130).
- Cox, G. F. and Weeks; W. F., 1983. Equations for determining the gas and brine volumes in sea ice samples. *Journal of Glaciology*, vol. 29, no. 102, pp. 306 – 316.
- Hoyland, K., 2007. Morphology and small-scale strength of ridges in the North-western Barents Sea. *Cold Regions Science and Technology*, vol. 48, no. 3, pp. 169-187.
- Moslet, P.O., 2007. Field testing of uniaxial compression strength of columnar sea ice. *Cold Regions Science and Technology*, vol. 48, no. 1, pp. 1-14.
- Richter-Menge, J. and Jones, K., 1993. The tensile strength of first-year sea ice. *Journal of Glaciology*, vol. 39, pp. 609-618.
- Sammonds, P., Murrell, S. and Rist, M., 1998. Fracture of multiyear sea ice. *Journal of geophysical research*, vol. 103, no. C10, pp. 21795-21815.
- Sand, B., Petrich, C. and Sudom, D., 2013, Morphologies of ridges surveyed off Svalbard and in Fram Strait, 2011 and 2012 Expeditions. *International Conference on Port and Ocean Engineering under Arctic Conditions*. Espoo, Finland (in print).
- Shafrova, S. and Høyland, K.V., 2008. Morphology and 2D spatial strength distribution in two Arctic first-year sea ice ridges. *Cold Regions Science and Technology*, vol. 51, no. 1, pp. 38-55.
- Strub-Klein, L. and Sudom, D., 2012. A comprehensive analysis of the morphology of first-year sea ice ridges. *Cold Regions Science and Technology*, vol. 82, pp. 94-109.
- Timco, G.W. and Frederking, R.M.W., 1990. Compressive strength of sea ice sheets. *Cold Regions Science and Technology*, vol. 17, no. 3, pp. 227-240.
- Timco, G.W. and Weeks, W.F., 2010. A review of the engineering properties of sea ice. *Cold Regions Science and Technology*, vol. 60, no. 2, pp. 107-129.
- WMO, 1970. WMO Sea ice nomenclature, (supplement No. 5, 1989). Tech. Rep. MO, no. 259. TP. 145, World meteorological Organization, Geneva, Switzerland.

## ACKNOWLEDGEMENT

This work was supported by the Research Council of Norway project number 195153.